(30) Burchard, W. *Br. Polym. J.* **1971**, *3*, 209.
(31) Franken, I.; Burchard, W. *Macromolecules* **1973**, *6*, 848.
(32) Yamakawa, H.; Fujii, M. *Macromolecules* **1974**, *7*, 649.
(33) Koyama, R. *J. Phys. Soc. Jpn.* **1973**, *34*, 1029.
(34) Burchard, W.; Schmidt, M.; Stockmayer, W. H. *Macromolecules* **1980**, *13*, 1265.
(35) Bantle, S.; Schmidt, M.; Burchard, W. *Macromolecules* **1982**, *15*, 1604.
(36) Stockmayer, W. H.; Schmidt, M. *Pure Appl. Chem.* **1982**, *54*, 407.
(37) Schmidt, M.; Stockmayer, W. H., in preparation.
(38) Fujime, S. *J. Phys. Soc. Jpn.* **1970**, *29*, 752.
(39) Fujime, S.; Maruyama, M. *Macromolecules* **1973**, *6*, 237.
(40) Maeda, T.; Fujime, S. *Macromolecules* **1981**, *14*, 809.
(41) Kubota, K.; Chu, B. *Macromolecules* **1983**, *16*, 105.
(42) Kubota, K.; Chu, B. *Biopolymers* **1983**, *22*, 1461.
(43) Harris, R. A.; Hearst, J. E. *J. Chem. Phys.* **1966**, *44*, 2595.
(44) Hearst, J. E.; Beals, E.; Harris, R. A. *J. Chem. Phys.* **1968**, *48*, 537.
(45) Schulz, G. V. *Z. Phys. Chem. (Leipzig)* **1939**, *43*, 25.
(46) Zimm, B. H. *J. Chem. Phys.* **1948**, *16*, 1099.
(47) Siegert, A. J. F. *MIT Rad. Lab.* **1943**, *Rep. No. 465*.
(48) Koppel, D. E. *J. Chem. Phys.* **1972**, *57*, 4814.
(49) Burchard, W. *Macromolecules* **1978**, *11*, 455.
(50) Schmidt, M.; Burchard, W. *Macromolecules* **1978**, *11*, 460.
(51) Burchard, W.; Schmidt, M.; Stockmayer, W. H. *Macromolecules* **1980**, *13*, 580.
(52) Mueller, M.; Burchard, W. *Int. J. Biol. Macromol.* **1981**, *3*, 71.
(53) Kirkwood, J. G.; Riseman, J. *J. Chem. Phys.* **1948**, *16*, 565.
(54) Broersma, S. *J. Chem. Phys.* **1960**, *32*, 1626.
(55) Yamakawa, H.; Fujii, M. *Macromolecules* **1973**, *6*, 407.
(56) Hearst, J. E.; Stockmayer, W. H. *J. Chem. Phys.* **1967**, *47*, 1396.
(57) Tanaka, G.; Stockmayer, W. H. *Proc. Natl. Acad. Sci. U.S.A.* **1982**, *79*, 6401.
(58) Berne, B.; Pecora, R. "Dynamic Light Scattering"; Wiley: New York, 1976.
(59) Rallison, J. M.; Leal, L. G. *J. Chem. Phys.* **1981**, *74*, 4819.
(60) Hagerman, P.; Zimm, B. H. *Biopolymers* **1981**, *20*, 1481.
(61) Marchal, E. *J. Chim. Phys.* **1966**, *63*, 1247.
(62) Dandliker, W. B.; Kraut, J. *J. Am. Chem. Soc.* **1956**, *78*, 2380.
(63) Provencher, S. W. *Comput. Phys. Commun.* **1982**, *27*, 213.
(64) Provencher, S. W. *Comput. Phys. Commun.* **1982**, *27*, 229.
(65) Schmidt, M.; Stockmayer, W. H.; Mansfield, M. *Macromolecules* **1982**, *15*, 1609.
(66) Imai, S. *J. Chem. Phys.* **1969**, *50*, 2116.
(67) Yamakawa, H. *J. Chem. Phys.* **1962**, *36*, 2995.
(68) Pyun, C. W.; Fixman, M. *J. Chem. Phys.* **1964**, *41*, 937.

Rotational Motion of the Ester Methyl Group in Stereoregular Poly(methyl methacrylate): A Neutron Scattering Study

Barbara Gabryś,* Julia S. Higgins, Karen T. Ma, and Jaan E. Roots

Department of Chemical Engineering and Chemical Technology, Imperial College, London SW7 2BY, England. *Received August 2, 1983*

ABSTRACT: Quasi-elastic neutron scattering data are reported for two stereoisomers of poly(methyl methacrylate) in which all but the ester methyl hydrogens have been replaced with deuterium. For syndio- and isotactic forms the observed motion is dominantly a threefold symmetric rotation about the O–CH_3 bond but the behavior in both cases is non-Arrhenius, with an apparent activation energy reducing from 7 kJ mol^{-1} above room temperature to 1 kJ mol^{-1} at 150 K. This behavior is explained by the inclusion of higher terms in the Fourier series expansion of the potential function for the methyl group rotation. Differences observed at lower temperatures in the absolute magnitude of the rotational rates for the stereoisomers are explained in terms of the relative angular phase of the threefold and higher Fourier terms in the potential.

1. Introduction

The intramolecular motion in polymers is manifested, for instance, in their dynamical-mechanical behavior.[1] Large-scale conformational rearrangements arising from rotations about backbone bonds are frozen in at the glass transition temperature, but even at lower temperatures there remain subsidiary loss mechanisms arising from the motion of side groups attached to the main chain. These latter motions have been identified not only in dynamic mechanical relaxation but also in dielectric relaxation,[1] NMR,[2-4] and neutron scattering.[5]

The barriers to rotation of methyl groups are relatively low compared to those of other side groups allowing a fairly fast rotational motion between sites, and the corresponding relaxation "peaks" are often difficult to observe in mechanical or NMR experiments because they occur as broad peaks at very low temperatures. The rather higher observation frequency of neutron scattering experiments together with the use of deuterium labeling has led to successful identification of methyl group libration within a potential well for a number of polymers via inelastic scattering,[6-9] and barrier heights to rotation have been calculated. Furthermore, the observation of rotational "hopping" over the barriers has been achieved via quasi-elastic scattering.[5,8]

The predominant effect on the rotational barriers of methyl side groups has been shown to be the chemical structure of the monomer unit, but in a few cases the stereoregularity produces a variation of 50% or more.[7] In the case of poly(methyl methacrylate) (PMMA) (Figure 1) the barrier height to rotation for the α-methyl group has been evaluated from inelastic neutron scattering (assuming that the observed frequency mainly corresponds to the 1–0 torsional transition within a threefold symmetric potential, V_3) and shown to vary from 23 kJ mol^{-1} for the isotactic form to 32 kJ mol^{-1} for the syndiotactic form.[7] Furthermore, activation energies as determined by NMR[4] vary from 15.5 to 22.6 kJ mol^{-1} for the two stereoisomers, respectively. If this increase is due to the nonbonded interactions between the α-methyl and the ester groups which are nearest neighbors in the syndiotactic PMMA (conformations of the two stereoisomeric forms of PMMA are shown in Figure 1), then a similar effect of stereoregularity might be expected also for the ester methyl group motions.

The torsional motion of the ester methyl group is observed in the inelastic neutron scattering spectrum to occur at a lower frequency than that for the α-methyl group,[6,7] indicating a lower barrier to rotation. The rotational hopping motion over this low barrier is correspondingly fast, allowing the motion to be well resolved in quasi-elastic neutron scattering experiments at low temperatures where all the other molecular motion has been frozen out. A measure of the barrier height may then be inferred from

0024-9297/84/2217-0560$01.50/0

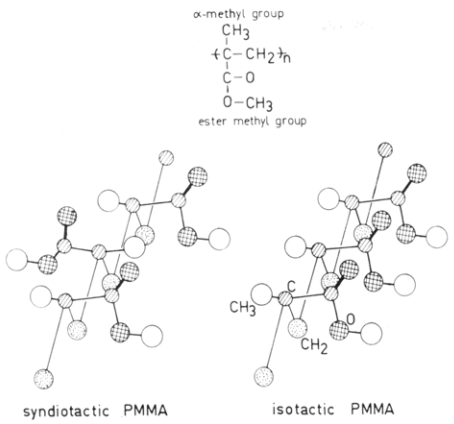

Figure 1. Chemical formula and schematic conformations for stereospecific forms of PMMA.

the temperature dependence of the observed rotational rate, assuming an Arrhenius dependence. The quasi-elastic neutron scattering experiments have the added advantage of providing simultaneously information of the geometry of the rotation. We report here therefore a study of the temperature dependence and geometry of the rotational motion of the ester methyl group in both isotactic and syndiotactic PMMA using quasi-elastic neutron scattering. Furthermore, inelastic neutron scattering results which give a more direct estimate of the barrier height to rotation are also reported.

2. Scattering from Polymeric Systems

The very large incoherent cross section of hydrogen means that in a system containing a high percentage of protons the total scattering cross section is dominated by the incoherent scattering of the protons;[10] the only important coherent scattered intensity is then concentrated in a few Bragg peaks or broader maxima. Therefore, it is generally a good approximation to consider only the motions of the protons.

Rotational motion of side groups (such as methyl groups) will not be the only contributor to incoherent neutron scattering from polymers. Torsional motion of these groups will give rise to inelastic scattering while rotation about side- and main-chain bonds will both be revealed in the quasi-elastic region.[10,11] Translation of the center of mass, although also quasi-elastic in nature, involves a time scale many orders of magnitude slower than rotations even in melt samples. In the present experiments, moreover, the samples are held below their glass transition temperatures so that even motion of short backbone sequences is frozen out and only side-group motion remains to contribute to the scattering.

If we assume that vibrational motion of protons about an average position and rotation around an axis are dynamically uncoupled, then the scattering law for vibrational motion can be expanded[10,12] in terms of the energy transfer, $\hbar\omega$, and it can be shown that the only vibrational contribution to the quasi-elastic scattering is through a Debye–Waller factor $\exp(-Q^2\langle u^2\rangle)$, where $\langle u^2\rangle$ is the mean square amplitude of vibration and Q is defined below. Thus

$$S_{\text{inc}}^{\text{qel}}(Q,\omega) = e^{-Q^2\langle u^2\rangle} S_{\text{inc}}^{\text{rot}}(Q,\omega) \tag{1}$$

$S_{\text{inc}}^{\text{qel}}(Q,\omega)$ is the scattering law for the sample in question for near-elastic events (quasi-elastic scattering) and $S_{\text{inc}}^{\text{rot}}(Q,\omega)$ is that for the rotational motion alone. Q is the magnitude of the scattering vector, which for near-elastic scattering is given by

$$Q = (4\pi/\lambda)\sin(\theta/2) \tag{2}$$

where λ is the wavelength of the incident neutrons and θ is the scattering angle. $S_{\text{inc}}^{\text{rot}}(Q,\omega)$ is given as a sum of a purely elastic component $A_0(Q)\delta(\omega)$ and a quasi-elastic component $S_{\text{rot}}^{\text{qel}}(Q,\omega)$[12,13]

$$S_{\text{inc}}^{\text{rot}}(Q,\omega) = A_0(Q)\delta(\omega) + S_{\text{rot}}^{\text{qel}}(Q,\omega) \tag{3}$$

The intensity of the elastic component, $A_0(Q)$, is called the elastic incoherent structure factor (EISF) and is a direct measure of the time-averaged spatial distribution of the proton; the Q variation gives information about the geometry (i.e., the overall symmetry) of the rotational motion. The quasi-elastic component contains the time evolution of the proton position, the frequency of rotation.

In order to calculate the form of $A_0(Q)$ and $S_{\text{rot}}^{\text{qel}}(Q,\omega)$, a model of the rotational motion must be made and the axis of rotation identified. In the case of the ester methyl group in PMMA, the motion is confined to a one-dimensional rotation about the O–CH_3 axis (it is generally assumed that the ester group is a planar structure[14] with the C=O group cis to CH_3; cf. Figure 1). Although there remains the possibility of a 180° flip about the C–C bond (see Figure 1), this is estimated to occur with a frequency of 1 Hz at 300 K,[15] which is well outside the range of the neutron experiments.

If the threefold symmetry of the methyl group itself is assumed to be the dominant factor in determining the angular variation of the rotational motion, then the motion can be considered in terms of "instantaneous" jumps between three equidistant sites on a circle of radius r.[16] For a powder sample the rotational scattering law can then be written as

$$S_{\text{inc}}^{\text{rot}}(Q,\omega) = A_0(Q)\delta(\omega) + \frac{1}{\pi}[1 - A_0(Q)]\frac{2\tau/3}{1 + \omega^2(2\tau/3)^2} \tag{4}$$

where τ is the mean time between two consecutive jumps and $A_0(Q)$ is given by

$$A_0(Q) = \frac{1}{3}[1 + 2j_0(3^{1/2}Qr)] \tag{5}$$

where $j_0(x)$ is the zeroth-order spherical Bessel function. The quasi-elastic component in eq 4 is a Lorentzian with a full width at half-maximum $(3/\tau)$ which is independent of Q. The mean residence time τ is usually assumed to follow an Arrhenius-type temperature dependence

$$\tau = \tau_0 \exp(E_a/k_B T) \tag{6}$$

where E_a, the activation energy, is essentially a measure of the height of the barrier between equivalent positions, k_B is the Boltzmann constant, and T is the absolute temperature.

A rotation of higher symmetry (for example, a sixfold rotation) would change $A_0(Q)$ and lead to an "effective" width of the quasi-elastic spectrum (measured with finite resolution) that increases with Q,[12,17] but details of the effect on the scattering law are left for discussion in subsequent sections.

3. Experimental Section

(a) Materials and Preparation of Samples. The monomer, methyl 2-(methyl-d_3)propenoate-3,3-d_2 (I) (CD_2=C(CD_3)-($COOCH_3$), was synthesized from perdeuterioacetone (99.5 atom % D) via acetocyanohydrin as described by Klesper et al.,[18] with the modification that the cyanohydrin was prepared essentially by the method in ref 19. NMR analysis of I showed the presence of $COOCH_3$ but also traces of CH_3 and CH_2, indicating that some hydrogen–deuterium exchange occurs during the synthesis; the selective deuteration is estimated to be of the order of 97%.

Thermal polymerization of I was carried out under gaseous N_2 at 50–55 °C using 2,2′-azobis(isobutyronitrile) as initiator to give

a product (PMMAS) which is predominantly syndiotactic. A stereospecific polymer (PMMAI) was obtained by polymerizing I in toluene at 0 °C with phenylmagnesium bromide as catalyst following the method by Goode et al.[20] Assuming the same stereoregularity as for fully hydrogeneous polymers prepared under identical conditions, NMR analysis indicates approximately 50% syndiotactic, 40% heterotactic, and 10% isotactic triads for PMMAS and nearly 100% isotacticity for PMMAI. Both polymers have very broad molecular weight distributions as determined by GPC (with polystyrene as standard) and peaks at ca. 2.5×10^5 (PMMAS) ca. 5.5×10^5 (PMMAI).

Samples were hot-pressed at approximately 120 °C into thin films of thickness calculated to give about 10% scattering (a compromise between reducing multiple scattering as far as possible and retaining sufficient intensity to obtain good counting statistics in reasonable time).

(b) Neutron Scattering. Neutron diffraction measurements were made at ambient temperature with the powder diffractometer 10H[21] at Harwell with an incident wavelength of 1.0 Å, giving a Q range of 0.8–11.4 Å^{-1}.

The inelastic and quasi-elastic data were all collected by using the time-of-flight spectrometer 4H5[21] at Harwell and the time-of-flight spectrometers IN5 and IN6[22] at the Institut Laue-Langevin, Grenoble. Measurements on 4H5 were made at ambient temperature while measurements on IN5 and IN6 covered the temperature range 150–390 K. Sample heating was achieved by using standard heating coils and a temperature controller (300–420 K, with temperature stability ±1 K); for cooling either a circulating refrigerator or a liquid helium cryostat was utilized (in each case, temperature control was within ±1 K).

For each of the spectrometers neutrons scattered by the sample were collected at a number of different scattering angles. For the inelastic measurements on 4H5 (incident wavelength of 6.0 Å), 13 angles between 13° and 90° were used. For the quasi-elastic measurements on IN5 and IN6, incident wavelengths of 4.8 and 5.1 Å, respectively, were used, giving scattering vector ranges of 0.3–2.3 and 0.3–2.0 Å^{-1}, respectively.

For each sample run, a corresponding empty sample can and vanadium standard run were made to allow background corrections and calibration of flight paths and detector efficiencies to be carried out and to determine the instrumental resolution. The resolution is strongly wavelength dependent for these time-of-flight instruments. Typically, the elastic resolution is of the order of 170 μeV (IN5) and in the range 80–150 μeV (IN6) at the wavelengths used. After the initial neutron counts in each time channel were corrected for detector efficiency and background effects were removed, neutron spectra were produced that were time-of-flight cross sections $\partial^2\sigma/\partial\Omega\,\partial\tau_n$ against τ_n at a fixed scattering angle, θ, where τ_n is the neutron "time-of-flight" and $\partial\Omega$ is an element of solid angle in the given direction.

(c) Data Analysis and Sources of Errors. The measured time-of-flight spectrum $\partial^2\sigma/\partial\Omega\,\partial\tau_n$ was converted into an experimental scattering law $S(Q,\omega)$ against energy transfer, $\hbar\omega$, via

$$S(Q,\omega) = \frac{4\pi\hbar}{\sigma_{sam}} \frac{k_0}{k} \frac{\tau_n^4}{\tau_{n0} m} \frac{\partial^2\sigma}{\partial\Omega\,\partial\tau_n} \tag{7}$$

where k_0 and k are magnitudes of the wavevector, τ_{n0} and τ_n are reciprocal velocities ("time-of-flight") for incident and scattered neutrons, respectively, and m is the neutron mass. σ_{sam} is the net incoherent scattering cross section for the scattering unit (conveniently a polymer repeat unit); σ_{sam} is usually taken as 1 since in the subsequent data analysis we do not need to correct the data by an absolute cross section. The symmetrized scattering law

$$\tilde{S}(Q,\omega) = \exp(-\hbar\omega/2k_BT)S(Q,\omega) \tag{8}$$

was the form used in the data analysis.

The inelastic spectrum, corrected as described above, may be related to the hydrogen amplitude weighted density of states, $g(\omega)$,[10] via

$$g(\omega) = \sinh(\hbar\omega/2k_BT)\frac{S(Q,\omega)}{Q^2}\frac{\hbar\omega}{k_BT} \tag{9}$$

Although an extrapolation to zero Q gives a result which is more directly comparable to infrared and Raman spectra, it has been found for spectral regions without strong dispersive effects that this extrapolation is unnecessary as well as being subject to large statistical errors.[8] Instead $g(\omega)$ can be summed over all scattering angles to improve the statistical accuracy, which was the procedure adopted in this study.

A model scattering law of the general form as given in eq 1 and 4 was fitted to the measured quasi-elastic $S(Q,\omega)$ data (corrected as described above) by using programs developed and described elsewhere.[23] The major steps in this procedure are the following:

(1) A model scattering law of unit area is calculated by using the starting parameters and scaled to fit the experimental scattering law; the variable quantities are effectively A_0, the half-width of the Lorentzian, and a scaling factor, which in our case includes the sample cross section (since σ_{sam} is taken as 1 in eq 7) and the Debye–Waller factor.

(2) A variable flat background is added which accounts for experimental inaccuracy in data correction for background scattering and, at high temperatures and high Q values, for the tail of the phonon spectrum in the wings. Furthermore, for broad quasi-elastic spectra the variation of Q across the peak is also taken into account.

(3) The model scattering law is converted to a time-of-flight spectrum with eq 7, convoluted with the resolution (vanadium) time-of-flight spectrum from which a flat background has been subtracted, and then reconverted to a scattering law. This maneuvre takes account of the finite instrumental resolution and avoids the uncertain deconvolution procedure occasionally adopted.

(4) The calculated function is compared to the experimental $\tilde{S}(Q,\omega)$ and an iteration using the four parameters in steps 1 and 2 is carried out until a best fit is obtained.

Although there are four variables used to fit the model scattering law to the experimental data, a number of internal consistency checks can be applied to the results since measurements were carried out at up to 19 different Q values. First, the flat background should be small, vary smoothly from angle to angle, and differ little from that observed in the measurement on vanadium. Second, for a simple threefold rotor the width ($\Delta\omega$) of the quasi-elastic component must be independent of Q (cf. eq 4), a condition which within experimental error was fulfilled for $Q \gtrsim 1$ Å^{-1}. (In this context it could be mentioned that there is very little quasi-elastic intensity at low Q values.) Finally, the evaluated $A_0(Q)$ must vary smoothly with Q, and $\Delta\omega$ should vary systematically with temperature.

Using these criteria one can achieve a high level of confidence in the fitted parameters. Figure 2 shows a typical fit attained at two Q values (T = 298 K) for PMMAS. In general, the error in the results obtained in the fitting procedure from the purely statistical uncertainty in the scattered neutron intensity was 5–10% of the value of the parameter.

A further contribution to the scattered intensity so far not considered is that from multiple scattering in the sample. Although this can be reduced as far as possible by keeping the total scattering cross section low, Monte Carlo calculations show that intensity still arises from this effect and approximately mirrors the overall shape of the first scattered spectrum. Hervet et al.[24] estimate the effect on the EISF to be no more than a few percent, while Richardson et al.[25] suggest an error up to 10%, especially at low Q. The error in $\Delta\omega$, which depends on the shape of the scattering law, will be rather less than that in the EISF. With these considerations in mind, extensive multiple-scattering corrections on the measured scattering laws were considered superfluous, although the samples were found to scatter about 25% of the incident neutrons.

4. Results

(a) Elastic Incoherent Structure Factor. An experimental estimate of the EISF, $M(Q)$, is obtained from the fitting program as the ratio

$$M(Q) = I_{el}/(I_{el} + I_{qel}) \tag{10}$$

where I_{el} and I_{qel} are the relative intensities of the elastic and quasi-elastic components, respectively. Figure 3 shows, as a function of Q, the values of $M(Q)$ obtained at two temperatures, each for both PMMA stereoisomers (for

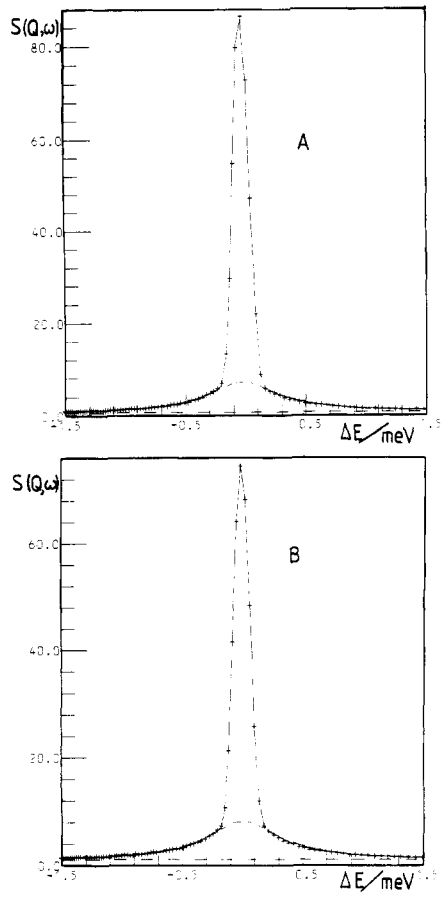

Figure 2. $S(Q,\omega)$ vs. energy transfer for PMMAS at 298 K: (A) Q = 1.36 Å^{-1}; (B) Q = 2.06 Å^{-1}.

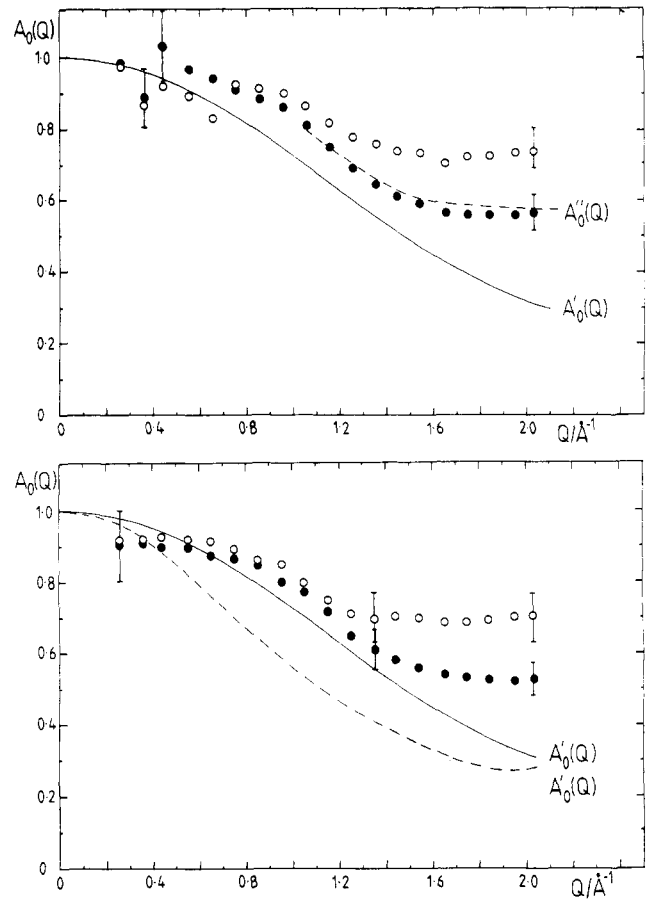

Figure 3. Elastic incoherent structure factor for (top) PMMAS at (○) 150 K and (●) 290 K and for (bottom) PMMAI at (○) 150 K and (●) 315 K. Solid line $A_0'(Q)$ is EISF calculated for a threefold rotation of the methyl group corrected for imperfect deuteration. Broken line $A_0''(Q)$ (top) is calculated EISF corrected for coherent scattering (see text). Broken line $A_0'(Q)$ (bottom) is EISF calculated for a combined threefold and twofold rotation (see text).

clarity, only the highest and lowest temperature data are included in Figure 3). Data obtained at intermediate temperatures fall systematically between these two limiting sets. An estimated error of 10% is included. The solid line in Figure 3 represents $A_0'(Q)$, the structure factor for a simple threefold rotator calculated according to eq 5, using a value of 1.032 Å for r and taking into account the incoherent contribution of the main chain and α-methyl deuterons and of a small fraction z of protons remaining due to imperfect deuteration of the sample. The procedure adopted for this correction follows the approach of Hervet et al.,[26] who give

$$A_0'(Q) = \frac{p_f}{p_f + p_m} + \frac{p_m}{p_f + p_m} A_0(Q) \tag{11}$$

where p_f and p_m represent the total number of fixed and mobile scattering centers, respectively, expressed in units of the hydrogen cross section and

$$\frac{p_f}{p_f + p_m} = \frac{\frac{5}{3}z + \frac{5}{3}(1-z)\frac{\sigma_D}{\sigma_H}}{1 + \frac{5}{3}z + \frac{5}{3}(1-z)\frac{\sigma_D}{\sigma_H}} \tag{11a}$$

In the present case NMR analysis indicates that z = 0.03. Thus

$$A_0'(Q) = 0.0864 + 0.9136 A_0(Q) \tag{12}$$

The calculated curve $A_0'(Q)$ in Figure 3 falls below the experimental data. The following arguments suggest that this is unlikely to be due to a wrong choice of either the axis of rotation or geometry. Leadbetter and Lechner[12] demonstrate that any increase in the number of sites above three for the rotational hopping reduces the value of $A_0(Q)$ at its first minimum. The dashed line in the bottom panel of Figure 3 is a calculation[8] of $A_0'(Q)$ following the method described by Dianoux et al.[27] for a complex rotation assuming a combination of a twofold flip of the whole ester group (radius r_1) about the C–C axis and a threefold rotation (radius r_2) about the O–CH_3 axis. The values of r_1 and r_2 based on bond angles and bond lengths[28] are 1.16 and 1.032 Å, respectively. The angle between the normal to the plane of the threefold rotation and the axis of the twofold flip is 4° for the energetically preferred ester group orientation (cf. Figure 1).

It is thus clear that the origin of the discrepancy between $A_0'(Q)$ and the data must be elsewhere. Figure 4 shows the observed coherent scattering compared to the isotropic incoherent scattering from the sample PMMAS measured with the diffractometer 10H at 298 K. This coherent contribution has not been taken into account in the calculation of $A_0'(Q)$. In the top panel of Figure 3 the dashed curve represents $A_0''(Q)$, which is $A_0'(Q)$ (solid line) corrected for this coherent scattering via

$$A_0''(Q) = \frac{A_0'(Q) + x(Q)}{1 + x(Q)} \tag{13}$$

where $x(Q)$ is the ratio of coherent to incoherent scattered intensity taken from Figure 4. There is good agreement between the calculated $A_0''(Q)$ and the experimental data obtained for the same sample of PMMAS at 290 K. Experimental limitations on the 10H diffractometer precluded measurements below 1.2 Å^{-1} so $A_0''(Q)$ has only

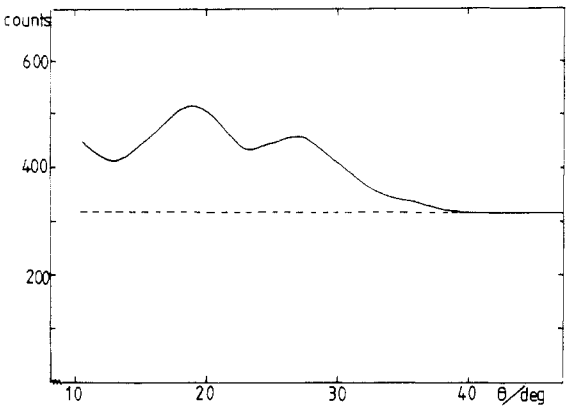

Figure 4. Structure factor for PMMAS at 298 K; counts against scattering angle. The dashed line is the assumed level of incoherent isotropic scattering. Statistical errors are given by $N^{1/2}$, where N is the neutron count.

Table I
Temperature Dependence of the Quasi-Elastic Spectral Widths and Rotational Frequencies for PMMAS and PMMAI

	fwhm/meV		$\nu_{rot}/10^{11}$ s^{-1}	
T/K	PMMAS	PMMAI	PMMAS	PMMAI
148	0.40 ± 0.04	0.27 ± 0.02	0.97	0.65
178		0.30 ± 0.01		0.73
205	0.50 ± 0.05	0.33 ± 0.01	1.21	0.80
249	0.59 ± 0.05	0.51 ± 0.01	1.43	1.23
262	0.64 ± 0.06		1.55	
290	0.74 ± 0.06	0.60 ± 0.02	1.78	1.45
298	0.84 ± 0.10		2.04	
298	0.70 ± 0.07		1.70	
314		0.75 ± 0.02		1.81
320	0.88 ± 0.06		2.13	
325	0.88 ± 0.08		2.13	
333	0.99 ± 0.08		2.39	
361	1.16 ± 0.10		2.81	
391	1.57 ± 0.16		3.80	

been calculated over the range of data shown in Figure 4. Although it has been shown that the main-chain structures (and hence coherent scattering patterns) are essentially similar for isotactic and syndiotactic stereoisomers,[28,29] the curve $A_0''(Q)$ has not been included in the bottom panel of Figure 3 for comparison with the isotactic PMMA data since the diffraction pattern was not observed directly for the sample PMMAI. Nevertheless, comparison of the top and bottom panels of Figure 3 shows that a similar correction to $A_0'(Q)$ would also produce close agreement between the calculated curve and the data for PMMAI at higher temperatures.

There remains the question of the origin of the systematic increase in the observed EISF as the sample temperature is reduced, which is well outside experimental error. The possible reasons for this increase will be discussed in section 5.

(b) Barrier to Rotation. Using the observation that the width of the quasi-elastic component fitted to the data is independent of Q for $Q \gtrsim 1$ Å^{-1}, we list the average over the higher Q values in Table I as the full width at half-maximum (fwhm) for the two stereoisomers at each temperature. The corresponding rotational frequencies (ν_{rot}) are also given in Table I. Figure 5 summarizes the temperature dependence of the fwhm on an Arrhenius plot. The behavior is clearly non-Arrhenius for both stereoisomers, with an apparent activation energy (cf. eq 6) falling from 7 kJ mol^{-1} above 300 K to 1 kJ mol^{-1} at 150 K. The possible reasons for this reduction are discussed in section 5.

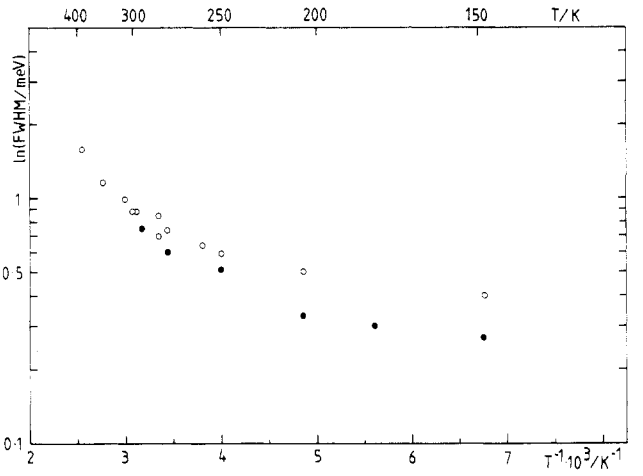

Figure 5. ln (fwhm) against T^{-1} from quasi-elastic scattering for (○) predominantly syndiotactic PMMA and (●) isotactic PMMA.

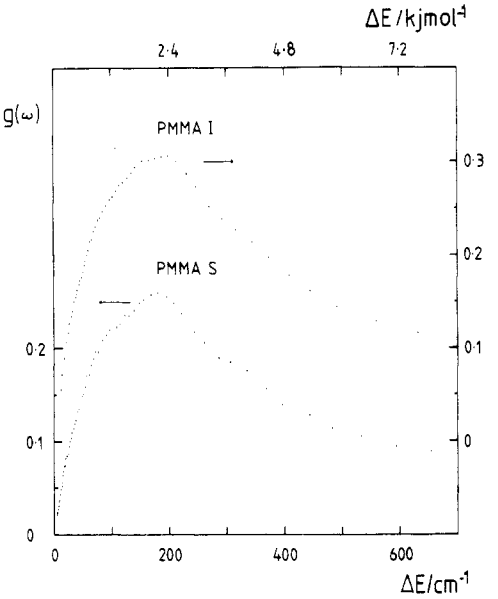

Figure 6. $g(\omega)$ summed over all scattering angles for both stereoisomers of PMMA.

Figure 6 shows the inelastic scattering from PMMAS and PMMAI at 298 K converted to the density of states $g(\omega)$ (cf. eq 9) and summed over all scattering angles. The comparison of normal coordinate analysis calculations with the far-infrared spectrum of PMMA[30,31] indicates that the region between 50 and 200 cm^{-1} is associated with motion in the ester group and with crystalline lattice modes. While the latter should display dispersion effects, no systematic shifts of peaks with scattering angle (or Q) were detectable in practice for these two samples of PMMA. Moreover, the large hydrogen amplitude in the methyl torsion suggests that this should produce an intense feature in the neutron spectrum,[6,7,9] and this optic mode is expected to show little dispersion. For these reasons no extrapolation of $g(\omega)$ to zero Q was attempted, and the broad peak centered around 180 cm^{-1} in both spectra in Figure 6 is assigned to the methyl group torsion. Application of a simple threefold cosine potential[32] and assuming the transition is predominantly 1–0 in character give an identical barrier height to rotation, V_3, for the two stereoisomeric forms of PMMA of 8.8 ± 1.9 kJ mol^{-1}.

5. Discussion

The rotational rates as a function of temperature (as represented in Figure 5) display two striking features.

First, the behavior is strongly non-Arrhenius and second, there is a distinct difference in the rotational rates for the two stereoisomers, especially at low temperatures. The limiting values of the apparent activation energy are 7 kJ mol^{-1} at high temperatures and 1 kJ mol^{-1} at low temperatures, and these values are closely similar for the two samples.

In order to explain these experimental observations, we propose the following model. It is customary to assume that methyl group rotation is hindered by a pure threefold cosine potential of the form

$$V(\alpha) = \frac{1}{2}V_3(1 - \cos 3\alpha) \quad (14)$$

where α is the angle of rotation about the C_3 axis and V_3 is the height of the barrier between the equivalent positions. V_3 can be calculated from the observed spectroscopic torsional transitions as quoted in section 4b. The activation energy E_a for rotation between sites will then be directly related to V_3, although some assumption about the energy of the ground state and the population of the higher torsional levels must be made. A simplistic view would indicate a reduction in the apparent E_a as temperature increases and the higher torsional levels become significantly populated. This model certainly cannot explain the apparently increasing barrier as temperature increases (cf. Figure 5) nor the differences in rotational rates between the stereoisomers since these are not accompanied by a change in E_a. If we assume a classical process as in eq 7, then the difference between the stereoisomers must lie in different values of the prefactor τ_0 if E_a does not change. τ_0, however, is usually assumed to depend on the torsional frequencies via the partition function, and for identical barriers τ_0 cannot change.

This is indeed the case when the methyl groups rotate independently of each other, and the symmetry of the potential is ascribed solely to the C_3 symmetry of the groups themselves. If, however, the higher terms in the Fourier series expansion are included, they may provide intermediate minima of much smaller depth than V_3 itself. Such minima would then give metastable angular sites for the methyl group protons as temperature decreases. The rotations observed would then correspond to the freeing of these intermediate states and would occur with much higher frequency than the rotations between the minima in V_3. (Extrapolation of the upper part of the curves in Figure 5 produces rotational rates unobservable at low temperatures in these experiments.) The similar slopes at low T in Figure 5 indicate that these intermediate minima should be of the same magnitude for the two stereoisomers. If, however, they occur at different angular phases relative to V_3 for the two structures, the overall shape of the potential is altered, and hence the distribution of energy levels, the partition function, and ultimately τ_0. Such an influence of local structure on the shape of the potential function has been observed for methyl groups substituted in different positions on a pyridine ring.[33] Low-temperature NMR and inelastic neutron scattering experiments show the potential for 2,6-dimethylpyridine is

$$V(\alpha) = \frac{1}{2}V_3(1 - \cos 3\alpha) + \frac{1}{2}V_6(1 - \cos 6\alpha) \quad (15)$$

while that for 2,5-dimethylpyridine is

$$V(\alpha) = \frac{1}{2}V_3(1 + \cos 3\alpha) + \frac{1}{2}V_6(1 + \cos 6\alpha) \quad (16)$$

In the case dealt with here, such an influence of local structure on the potential function is more likely to come from the different electron repulsion of the oxygen atom in the two PMMA stereoisomers than from the other methyl groups (cf. Figure 1).

This model also explains the observed temperature dependence of the structure factor. The top panel of Figure 3 shows that an excellent agreement is achieved between the calculated and observed structure factor for PMMAS at 290 K when both the imperfect deuteration and the coherent scattering contributions are accounted for. This result confirms the initial assumption about the geometry of the motion; i.e., rotation about the O–CH_3 axis and the threefold symmetry of the methyl group itself are dominant in determining the angular variation of the motion. It appears from comparison with the bottom panel of Figure 3 that a similar agreement would be obtained at higher temperatures for isotactic PMMA. As the temperature is reduced, however, for both stereoisomers there is a systematic increase in the values of the observed EISF, especially at higher Q values. The differences is as large as 30% between 325 and 150 K.

The freeing of the intermediate rotational states with decreasing temperature, as discussed above, causes the methyl group rotation to be dominated by the proton "jumps" over the lower barrier. Since the corresponding potential minima are localized over much smaller distance than those corresponding to the higher barriers, this will result in an increase of the EISF values and shift its first minimum in Q toward the higher Q values (cf. Figure 8.1 of ref 12). It is worthwhile recalling that for a given model, the structure factor is independent of temperature (cf. eq 5). In order to explain the observed increase in the structure factor while allowing 360° rotations, an unphysical reorientation of the methyl group between two equivalent sites would have to be proposed since only a reduction in the number of equivalent sites increases $A_0(Q)$.[12] The bottom panel of Figure 3 shows, moreover, that a combined threefold/twofold rotation reduces $A_0(Q)$.

An alternative explanation of the temperature dependence of the structure factor would center on the ratio $x(Q)$ of coherent to incoherent cross sections within the sample (vide supra). In order to explain the observed changes one has to analyze the temperature dependence of eq 13 and thus the temperature dependence of the *ratio* of the coherent to incoherent scattering. The dominant incoherent scattering centers are the highly mobile ester methyl group hydrogens, and a decrease of their cross section with temperature could be expected. The coherent cross section, dominated mainly by backbone or deuterated α-methyl group scatterers is expected to change little with temperature due to their low mobility. If the extreme assumption of an invariant σ_{coh} and a changing σ_{inc} is made, then the latter would have to reduce by 55% over the range from 325 to 150 K to explain the data.

It is known that the total cross section of hydrogeneous molecules increases either with decreasing energy of the incident neutrons or with increasing temperature of the scattering molecules.[34] Changes of the order of 50% or more have been observed in the neutron transmission of polystyrene and of polybutadiene over a temperature range of 150 K,[35] but at higher temperatures than quoted here. In view of the preceding arguments, this explanation seems to be less likely than the former.

Non-Arrhenius behavior of relaxation rates such as shown in Figure 5 has previously been explained as a quantum effect. It is noticeable that the shape of the curve in Figure 5 bears a strong resemblance to the calculated temperature dependence of the quantum mechanical tunneling frequency averaged over all torsional states of the methyl group.[36] Thus an explanation of the observed fast motion at low temperatures in terms of quantum mechanical tunneling through the potential barrier would

appear plausible in that tunneling can be the dominant reorientation mechanism at low temperatures.[37] Unfortunately, this explanation is not valid since it has recently been shown both experimentally[38] and theoretically[39] that the tunneling frequency decreases with increasing temperature and is in practice not observable above 70 K. A detailed discussion of the effects of quantum mechanical tunneling on the observed rotations of methyl groups is beyond the scope of this paper and will be dealt with elsewhere.[40] It is nevertheless clear that such effects cannot explain the data in Figure 5.

The disordered nature of the polymer samples probably precludes very detailed analysis of the shape of the potential barriers, but nonetheless experiments at low temperatures and particularly spectroscopy of the torsional levels should be instructive.

6. Conclusions

The rotational motion of the ester methyl groups in PMMA can be satisfactorily explained at ambient temperature in terms of a purely threefold cosine potential. At low temperatures a much higher rotational rate is observed than can be predicted by an Arrhenius-type extrapolation from rates observed at ambient temperature. This effect can be explained if the potential contains terms of higher order in the Fourier series expansion so that minima at intermediate angles and of much smaller depth than V_3 provide metastable positions for the methyl group protons. The differences observed at low temperatures in absolute rotational rate but not in apparent activation energy between the stereoisomers are believed to arise because of the different angular phase of the higher symmetry terms with respect to the threefold term. This is then one of the few cases observed of structure (in terms of nearest neighbors) affecting the potential to rotation of methyl groups.

Acknowledgment. We are indebted to the Science and Engineering Research Council for Research Fellowships (to B.G., K.T.M., and J.E.R.). Our understanding of these results has been deepened following discussion with Prof. A. Hüller and we express our gratitude. We thank Dr. R. Hall for the synthesis of the partially deuterated polymers, Drs. R. Ghosh and A. Maconnachie for help with the measurements, and Mr. K. Knowles for assistance with the computational work. We gratefully acknowledge the use of the experimental facilities at the Institut Laue-Langevin.

Registry No. PMMAI, 25188-98-1; PMMAS, 25188-97-0; neutron, 12586-31-1.

References and Notes

(1) McCrum, N. G.; Read, B. E.; Williams, G. "Anelastic and Dielectric Effects in Polymeric Solids"; Wiley: New York, 1967.
(2) Kawai, T. *J. Phys. Soc. Jpn.* **1961**, *16*, 1220.
(3) Powles, J. G.; Strange, J. H.; Sandiford, D. J. H. *Polymer* **1963**, *4*, 401.
(4) Connor, T. M.; Hartland, A. *Phys. Lett.* **1966**, *23*, 622.
(5) Allen, G.; Higgins, J. S. *Macromolecules* **1977**, *10*, 1006.
(6) Higgins, J. S.; Allen, G.; Brier, P. N. *Polymer* **1972**, *13*, 157.
(7) Allen, G.; Wright, C. J.; Higgins, J. S. *Polymer* **1974**, *15*, 319.
(8) Ma, K. T. Ph.D. Thesis, Imperial College, 1981.
(9) Takeuchi, H.; Higgins, J. S.; Hill, A.; Maconnachie, A.; Allen, G.; Stirling, G. *Polymer* **1982**, *23*, 499.
(10) Allen, G.; Higgins, J. S. *Rep. Prog. Phys.* **1973**, *36*, 1073.
(11) Higgins, J. S. In "Developments in Polymer Characterisation"; Dawkins, J. V., Ed.; Applied Science Publishers Ltd.: Barking, Essex, 1983; Vol. 4.
(12) Leadbetter, A. J.; Lechner, R. E. In "The Plastically Crystalline State"; Sherwood, J., N., Ed.; Wiley: New York, 1979.
(13) Volino, F.; Dianoux, A. J. In *Proc. Euchem. Conf. 1976* **1979**.
(14) Havrilak, S.; Roman, N. *Polymer* **1966**, *7*, 387.
(15) Reference 1, Chapter 8.
(16) Barnes, J. D. "Neutron Inelastic Scattering"; IAEA: Vienna, 1972; p 287; *J. Chem. Phys.* **1973**, *58*, 5193.
(17) Springer, T. *Springer Tracts Mod. Phys.* **1972**, *64*.
(18) Klesper, E.; Johnsen, A.; Gronski, W.; Wehrli, F. W. *Makromol. Chem.* **1975**, *176*, 1071.
(19) "Organic Syntheses"; Wiley: New York, 1955; Collect. Vol. III, p 324.
(20) Goode, W. E.; Owens, F. H.; Fellman, R. P.; Snyder, W. H.; Moore, J. E. *Am. Chem. Soc., Div. Paint, Plast. Printing Ink Chem., Prepr.* **1959**, *19*, 134.
(21) Baston, A. H., Harris, D. H. C., Eds. "Neutron Beam Instruments at Harwell", AERE-R9278, 1978.
(22) "Neutron Beam Facilities Available for Users", Institut Laue-Langevin, 38042 Grenoble, France.
(23) Richardson, R. M. "Notes on Some Quasielastic Scattering Analysis Programs on the Rutherford Laboratory IBM 360/195", RL-79-095, 1979.
(24) Hervet, H.; Volino, F.; Dianoux, A. J.; Lechner, R. E. *Phys. Rev. Lett.* **1975**, *34*, 451.
(25) Richardson, R. M.; Leadbetter, A. J.; Bonsor, D. H.; Krüger, G. J. *Mol. Phys.* **1980**, *40*, 741.
(26) Hervet, H.; Dianoux, A. J.; Lechner, R. E.; Volino, F. *J. Phys. (Paris)* **1976**, *37*, 587.
(27) Dianoux, A.; Volino, F.; Hervet, H. *Mol. Phys.* **1975**, *30*, 1181.
(28) Sundararajan, P. R.; Flory, P. J. *J. Am. Chem. Soc.* **1974**, *96*, 5021.
(29) Lovell, R.; Windle, A. H. *Polymer* **1981**, *22*, 175.
(30) Tadokoro, H.; Chatani, Y.; Kusanagi, H.; Yokoyama, M. *Macromolecules* **1970**, *3*, 441.
(31) Mandley, T. R.; Martin, C. G. *Polymer* **1971**, *12*, 524.
(32) Lin, C. C.; Swalen, J. D. *Rev. Mod. Phys.* **1959**, *31*, 841.
(33) Müller-Warmuth, W.; Schuler, R.; Prager, M.; Kollmar, A. *J. Chem. Phys.* **1978**, *69*, 2382.
(34) Janik, J. A.; Kowalski, A. In "Thermal Neutron Scattering"; Egelstaff, P. A., Ed.; Academic Press: New York, 1965; Chapter 10.
(35) Maconnachie, A., to be published.
(36) Stejskal, E. O.; Gutowski, H. S. *J. Chem. Phys.* **1958**, *28*, 388.
(37) White, J. W. In "Dynamics of Solids and Liquids by Neutron Scattering"; Lovesey, S. W., Springer, T., Eds.; Springer-Verlag: West Berlin and Heidelberg, 1977; Chapter 4.
(38) Cockbain, J. R.; Lechner, R.; Owen, M.; Thomas, R. K.; White, J. W. *Mol. Phys.* **1982**, *45*, 1035 and references therein.
(39) Hewson, A. C. *J. Phys.* **1982**, *15*, 3855 and references therein.
(40) Gabryś, B.; Higgins, J. S., to be published.